Chapter–3

Heat transfer modeling of improved biomass cook stove

Chapter 3

Heat transfer modeling of improved biomass cook stove

3.1 Introduction

Biomass cook stove is a thermal conversion device with complex network of heat transfer processes. Modeling techniques can be used to assess change in heat transfer within a stove with probable changes in stove design and operational procedure [1-2]. The heat transfer models are developed either for steady or unsteady state conditions where fuel, air, combustion, flame, stove and pot are important system components [1]. The models could predict the thermal output and also helpful for optimization of design parameters [3] which in turn affect the stove's performance. Artificial neural network [4-6], computational fluid dynamics [6-10] and fluent [6, 9] are some of the common tools used in modeling of stove. Use of such tools not only improves predictability but also increases the degree of accuracy provided models realistically represent minute details and variability. However, heat transfer model of biomass cook stove as integration of delineated systems has been limited. Therefore, in this present work of development of improved cook stove, attempt is made to disintegrate the biomass cook stove into specific components based on the network of heat transfer and subsequently steady state heat transfer models are developed for each of identified components. Finally, five parameters of the stove namely, ignition front velocity, burn rate, power delivery, efficiency and time to boil are modeled [1-2] in terms host of system parameters concerning design, materials, fuel and mode of air supply [2]. The details of the model development procedure and models are presented below.

3.2 Assumptions for steady state heat transfer modeling

Working of a biomass cook stove follows the stages of initial stage, operational stage and post-operational stage. The power output during initial stage increases up to the rated value and started decreasing during post-operational stage up to nil. Thus, both the initial and final stages are transient in nature. Uniform power output with little or no variation *i.e.*, steady state, is desired during operational phase. Thus, in the present study, performance modeling corresponding to steady state operational phase for a short time interval during operation is considered without feedback. The relevant assumptions for development of the models are listed as below:

a) Primary air flow is uniform and non-homogeneity of fuel is ignored.
b) The combustion occurs on the top face of the fuel bed with depth equal to a particle's height, whereas the rest of the fuel bed is at a uniform temperature lower than ignition temperature.
c) Dry air from the ambient is used for combustion.
d) Molar ratio between nitrogen and oxygen is considered as 3.76 [11].
e) Presence of argon in the combustion air has no effect on combustion process [11].
f) Temperatures at various sections of the stove are steady but different.
g) Fuel wood particles with less than 30% moisture are considered.
h) The fuel particles are distributed in honeycomb pattern and combustion is complete.
i) Nucleate Pool Boiling condition with excess water temperature (ΔT_e) is equal to 5°C is considered.

During combustion, the flame and the igniting fuel bed are the sources of heat for all remaining components of heat as depicted in Fig. 3.1 and listed in Table 3.1. As shown in Fig. 3.1, the air for combustion is sucked through the grate and passes through narrow channels located inside the bed. Reduction in air flow regime has been reported in earlier studies too [1]. However, in the present study the shape and size of the channels are modeled based on the shape and size of the fuel particles. Assumptions have been made that the fuel particles as well as the gaps are uniformly distributed within the fuel bed throughout stove cross-section.

Table 3.1: Heat transfer components inside the stove

Symbols	**Heat transfer component**	**Mode of heat transfer**
Q_1	Fuel bed to primary air at gaps	Convection
Q_2	Fuel bed to primary air envelope	Radiation
Q_3	Flame to fuel bed	Conduction + Radiation
Q_4	Fuel bed to bottom layer	Conduction
Q_{4a}	Heat received by primary air to reach ignition temperature	Heat used to raise the temperature from room temperature to ignition temperature
Q_{4b}	Heat lost by lower bed to ambient through grate	Radiation
Q_{4c}	Heat used for moisture to evaporate	Loss
Q_5	Flame to excess air	Conduction
Q_6	Flame to combustion chamber inner wall	Radiation
Q_7	Fuel bed to combustion chamber inner wall	Radiation
Q_8	Radiation heat from flame to pot	Radiation
Q_9	Fuel bed to pot	Radiation
Q_{10}	Combustion chamber inner wall to excess air	Convection

Symbols	Heat transfer component	Mode of heat transfer
Q_{11}	Combined heat transfer from flame and combustion chamber to excess air	Radiation
Q_{12}	Combustion chamber inner wall to pot bottom	Radiation
Q_{13}	Combustion chamber outer wall to surrounding	Radiation + Convection
Q_{14}	Convection heat from flame to pot	Convection
Q_{15}	Flue gas to pot bottom	Convection
Q_{16}	Flue gas to pot side surface	Convection
Q_{17}	Flame to surrounding	Radiation
Q_{18}	Heat carried by flue gas to ambient	Loss
Q_{19}	Unburned charcoal	Charcoal
Q_{20}	Heat lost by pot to surrounding	Convection + Radiation
Q_{21}	Heat used by water to reach boiling point	Convection
Q_{22}	Heat used to evaporate water from pot	Evaporation

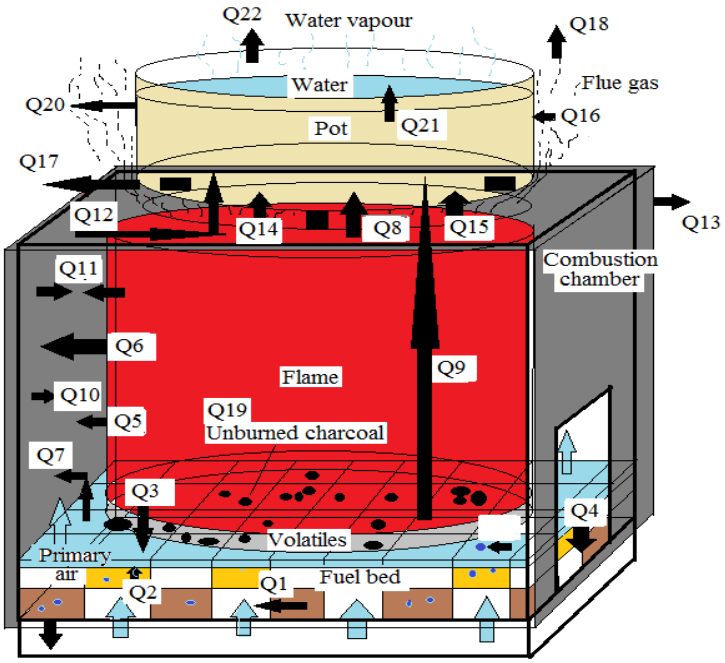

Fig.3.1: Schematic diagram of stove operation showing different heat transfer components

3.3 Heat transfer components

During combustion Q_{com} heat is released, which is the product of burning rate ($\dot{m}$) and the net calorific value (NCV) of fuel. It is the combination of heat which is subsequently released from flame (Q_f) and fixed carbon (Q_{fc}) to distinct networks of heat transfer. The entire network of heat transfer as described in Fig. 3.1 and listed in Table 3.2 are assessed through fundamental relationships obtained as a sole or combination of different modes *i.e.* conduction, convection and radiation. For each of the aspects considered within the stove, energy balance is conceptualized in terms of

the net total heat (Q_{total}), conductive heat (Q_{cond}), convective heat (Q_{conv}) and radiation heat (Q_{rad}) as in Eq. 3.1.

$$\pm Q_{total} = \pm Q_{cond} \pm Q_{conv} \pm Q_{rad} \quad 3.1$$

Fundamental heat transfer relationships as provided in Eq. 3.2 to Eq. 3.4 are used to model different components of heat transfer

$$Q_{cond} = kA_{cond}(\Delta T/\Delta x) \quad 3.2$$

$$Q_{conv} = hA_{conv}\Delta T \quad 3.3$$

$$Q_{rad} = FA_{rad}\varepsilon\sigma(T_{max}^4 - T_{min}^4) \quad 3.4$$

3.3.1 Modeling ignition front velocity, burn rate and power delivery

The combustion process as given in Eq. 3.5 is used to estimate air and flue gas flow rates during stove operation.

$$\left(\frac{a}{12}C + \frac{b}{2}H_2 + \frac{c}{28}N_2 + \frac{d}{32}O_2\right) + x(O_2 + 3.76N_2)(1+\psi) \rightarrow p\ CO_2 + q\ H_2O + r\ N_2 + x \times \psi(O_2 + 3.76N_2) \quad 3.5$$

where,

$$x = \frac{1}{3.76}\left(\frac{a \times I}{12 \times F} - \frac{c}{28}\right) \quad 3.6$$

$$r = (a/12) \times (I/F) \quad 3.7$$

where *a*, *b*, *c* and *d* represents elemental composition *i.e.*, *C*, H_2, N_2, and O_2, respectively of the fuel in mass percentage; *F* and *I* are composition of CO_2 and N_2 in flue gas (mass percentage) respectively, whereas values of *p* and *q* are *a*/12 and *b*/2 respectively. Terms on the left hand side of Eq. 3.5 represents the elemental composition of fuel and air required respectively, whereas terms on the product side represents the flue gas composition. Thus, theoretical air requirement is estimated from the knowledge of the elemental composition of fuel, however estimation of excess air needs the knowledge of draft created. Further, the relationships provided in Saastamoinen et al., [2] are used to determine ignition front velocity (w_{ig}) as given below

$$w_{ig} = q_{ig}/Q" \quad 3.8$$

where the heat flux (q_{ig}) is a function of flame temperature (T_f) and the radiation coefficient (K_R) as provided in Eq. 3.9, Eq. 3.10 and Eq. 3.11 respectively [2]

$$q_{ig} = K_R \sigma T_f^4 \quad 3.9$$

$$T_f = b_0 + b_1 m_g - b_2 m_g^2 \quad 3.10$$

$$K_R = a_0 - a_1 m_g \quad 3.11$$

where coefficients a_0 (0.2), a_1 (2), b_0 (903), b_1 (5547) and b_2 (11626) may be considered from literature [1-2] resembling woody biomass, m_g is the air flux determined as the product of air velocity and the air density. During combustion the top layer of fuel bed is at ignition mode and is at an average temperature (T_{fb}) of T_f and T_{ig}. The fuel particles are assumed to be uniformly distributed along the fuel bed whose shape and size also affects the gap shape and size. The velocity of air (V_a) flowing through the gaps of fuel bed is determined through iteration that matches the experimental values of ignition front velocity (w_{ig}), as reported [1] for similar configuration of stove.

The value of energy per unit volume of fuel, Q'' is determined as the sum of energy used to ignite fuel as well as energy used to evaporate fuel moisture as in Eq. 3.12 [2].

$$Q" = (1-\varepsilon)\rho_{fuel}\{c_{p,fuel}(T_{ig} - T_\infty) + y_m[\lambda + c_{p,w}(T_w - T_\infty)]\} \quad 3.12$$

The burn rate ($\dot{m}$) and power delivery (Q_{com}) of the stove are determined using Eq. 3.13 and Eq. 3.14 below.

$$\dot{m} = w_{ig} \times \rho_{bulk} \times A_b \quad 3.13$$

$$Q_{com} = \dot{m} \times NCV \quad 3.14$$

3.3.2 Heat transfer analysis of fuel bed and combustion chamber

As the combustion propagates the combustion chamber temperature rises creating a natural draft inside it. The air for combustion thus is sucked through the gaps located inside the fuel bed. During its passage through the fuel bed the air receives heat from the fuel bed through both convection (Q_1) and radiation (Q_2). Determination of the

convective heat transfer (Q_1) requires the estimation of exposed area, fuel bed temperature and convective coefficient (h_{pa_fb}) as in Eq. 3.3. These gaps are surrounded by low heat conducting hot walls on four sides and therefore resembles version 4 for H2 boundary condition [12] as listed in Table C.1 of Appendix C [12]. Thus Nusselt number for determination of convective coefficient (h_{pa_fb}) is obtained from reported results which depend on the aspect ratio of the duct and air flow conditions. The hydraulic diameter (D_h) of the ducts whereas could be determined as the ratio of four times the cross-sectional area (A_C) and wetted perimeter (P) of ducts. Whereas after passing through the fuel bed the combustion air forms a layer over the fuel bed at ignition temperature and receives heat through radiation mode from the fuel bed (Q_2) as in Eq. 3.4.

The top igniting layer, in a subsequent process, transfers heat to the fuel particles located beneath it through conduction mode (Q_{4a}). The heat transferred to the lower fuel bed is subsequently transferred to the air passing through the bed to increase its temperature to the ignition point of the volatiles (T_{ig}) as in Eq. 3.15.

$$Q_{4a} = \int_{T_\infty}^{T_{ig}} \sum n_i c_{p,i}\, dT \qquad 3.15$$

where, n_i and $c_{p,i}$ are the rate of formation and coefficient of specific heat of i^{th} gas species in primary air respectively. The present study considers the presence of O_2 and N_2 only in air. The values for n_{N_2} and n_{O_2} could be estimated as in Eq. 3.16 and 3.17.

$$n_{N_2} = r + x \times \psi \times 3.76 \qquad 3.16$$

$$n_{O_2} = x \times \psi \qquad 3.17$$

Values for $c_{p,i}$ could be estimated as in Eq. 3.18 considering gas specific coefficients i.e. *a*, *b*, *c* and *d* as in Table 3.2 [1].

$$c_p = a + bT + cT^2 + dT^3 \qquad 3.18$$

Table 3.2: Constants of heat capacity equation for gas species [1]

Compound	***a***	***b*×10^3**	***c*×10^6**	***d*×10^9**
CO_2	21.3655	64.2841	-41.056	9.7999
H_2O	32.4921	0.0796	13.2107	-4.5474
N_2	29.5909	-5.141	13.1829	-4.968
O_2	26.0257	11.7551	-2.3426	-0.05623

In a subsequent process the lower surface of the bottom fuel bed is exposed to the ambient and losses (Q_{4b}) radiation heat to ambient through the grate as in Eq. 3.4. View factor of the bottom surface of fuel bed is considered unity with respect to the ambient, as all the heat emitted is assumed to be transferred to the ambient and the presence of any other heat sharing surfaces is neglected. In addition to above two heat transfer processes, a part of the heat is also utilized by the bottom fuel particles to evaporate the moisture (Q_{4c}) within the fuel particles as a fuel preparation process prior to ignition. The heat utilized for moisture removal (Q_{4c}) is determined as the product of λ (latent heat of vaporization of water, 2441 kJ/kg) and m_{mc} (amount of moisture).

3.3.3 Heat transfer analysis from flame

During combustion, parts of heat from both flame as well as igniting fuel particles are transferred to the unburned particles. The flame transfers (Q_3) amount of heat to the fuel bed through both conduction (Q_{3a}) and radiation mode (Q_{3b}). The conduction heat transfer ($Q3_a$) from the flame could be determined as in Eq. 3.19.

$$Q_{3a} = k_{vol} A_{FB} \left(T_f - T_{FB}\right) / x_{vol} \tag{3.19}$$

where k_{vol} is the volatile layer thermal conductivity as in Eq. 3.20, A_{fb} is the fuel bed area, T_f is the flame temperature, T_{fb} is the fuel bed temperature and x_{vol} is the thickness of volatile layer.

$$k_{vol} = \frac{\sum_{i=1}^{i=n} k_i}{n} \tag{3.20}$$

where k_i is the thermal conductivity of individual volatile component obtained from literatures and n is the number of components considered. On the other hand heat transfer through radiation (Q_{3b}) from flame to fuel bed could be determined as in Eq. 3.21 [13].

$$Q_{3b} = F_{fb} A_f \varepsilon_f \sigma T_f^4 (1 - exp^{-kx}) \tag{3.21}$$

where, F_{fb}, A_f, T_f , k, x and ε_f are the view factor, flame area, flame temperature, decay coefficient (0.7322 m^{-1}) [13], flame thickness and emissivity of the flame. Both the flame and fuel bed are of equal radius r_b and is separated by distance H_{fb}. Thus the view factor (F_{fb}) between the flame and the fuel bed is calculated as in Eq. 3.22 [14].

$$F_{fb} = \frac{1}{2}\left\{\left(1+\frac{1+R^2}{R^2}\right) - \left[\left(1+\frac{1+R^2}{R^2}\right)^2 - 4\right]^{1/2}\right\}; R = \frac{r_{fb}}{H_{fb}} \quad 3.22$$

The emissivity of flame changes with change in its height. As per the literatures two different correlations could be used for determination of flame emissivity at 1/4th and 3/4th of flame height [15]. As the fuel bed is nearest to 1/4th flame height, therefore emissivity could be determined from Eq. 3.23 [15].

$$\varepsilon_f = 1 - exp^{-3.11x} \quad 3.23$$

The pot's outer surface consists of two connected portions i.e. pot bottom and pot side surface. However heat received by both these surfaces differs due to variation in exposure to different heat transferring bodies or components.

Similarly, as the flame moves upwards the pot's outer surface comes in contact with the hot flame and flue gas. Thus, the pot's outer surface at temperature T_{pb} receives heat from the flame and the flue gas. The flame transfers both radiation (Q_8) as well as convection heat (Q_{14}) to the pot's outer surface, whereas the flue gas transfers heat through convection to the pot bottom (Q_{15}), its side wall (Q_{16}) and carries a part to the ambient (Q_{18}). Radiation heat transfer from the flame to the pot is discussed in Section 3.5. The effect of flue gas radiation effect is neglected. The convective heat transfer components i.e. Q_{14}, Q_{15} and Q_{16} could be determined using the correlation as in Eq. 3.3. Convective coefficient of flame is considered to be 28.39 W/m^{2}K for all cases [13]. Similarly convective coefficient of flue gas passing over the pot bottom is determined using Eq. 3.24 and Eq. 3.25 considering pot as normal to flow direction of flue gas.

$$h = \frac{Nu \times k}{r_{pb}} \quad 3.24$$

where, r_{pb} and k are the pot radius and flue gas thermal conductivity at temperature T_{fg} which is the average of pot and flame temperature. The Nusselt number of flue gas flowing over the pot surface is determined as Eq. 3.25 [16]

$$Nu = 0.714\, Re^{1/2} Pr^{1/3} \quad 3.25$$

where, Re and Pr are the Reynold's Number and Prandtl Number which could be determined as in Eq. 3.26 and Eq. 3.27 respectively.

$$Re = \rho VL/\mu \quad (3.26)$$

$$Pr = \mu c_p/k \quad (3.27)$$

where ρ, V, L, μ, c_p and k are the density, velocity, length of travel, dynamic viscosity and thermal conductivity of flue gas. The values for ρ, μ, c_p and k could be obtained from the thermo physical properties chart as provided in Appendix D [17].

While the flow of flue gas over the side wall of the pot could be determined using Eq. 3.28 [18] considering flow over a flat plate.

$$h = \begin{cases} 3.83\, V^{0.5} L^{-0.5}\ (Laminar\ flow) \\ 5.74\, V^{0.8}\, L^{-0.2}\quad (Fully\ turbulent\ flow) \\ 5.74\, V^{0.8} L^{-0.2} - 16.46\, L^{-1}\ (Mixed\ flow) \end{cases} \quad (3.28)$$

where, V and L are the velocity of flue gas and length of travel equal to pot's height respectively. However, suitability of the condition depends on the Reynolds number of the flue gas. After transferring heat to the pot, the flue gas is released to the ambient consisting Q_{18} heat in it as determined from Eq. 3.15. The flue gas is considered to be composed of O_2, N_2, CO_2 and H_2O and is represented by i in Eq. 3.15. Values of n_i for various gas components could be determined from earlier discussions, whereas for CO_2 and H_2O the elemental analysis is estimated from fuel such that rate of formation of carbon dioxide (n_{CO_2}) and water (n_{H_2O}) are represented by p and q. The value for $c_{p,i}$ corresponding to the gas species (O_2 and N_2) could be determined as in Eq. 3.18 and Table 3.2 [1]. During the process of heat transfer by the flame to the pot's outer surface the flame is exposed to the ambient at the gap between the combustion chamber and the pot bottom. The flame therefore losses (Q_{17}) heat through radiation to the ambient as in Eq. 3.21. As the heat loss occurs at the top portion of the flame, therefore emissivity is considered to be equal to that at 3/4th flame height as in Eq. 3.29 [15].

$$\varepsilon_f = 1 - exp^{-2.24x} \quad (3.29)$$

where, x is the flame thickness.

3.3.4 Heat transfer analysis of combustion chamber

The considered combustion chamber is assumed to be metallic having melting point higher than the flame temperature with smoother inner and outer walls. The outer wall

is assumed to be exposed to surrounding whereas the inner wall is exposed to flame, flue gas, excess air and fuel bed. The combustion chamber maintains a lower thickness to diameter ratio which is assumed to be uniform through its height. During combustion the combustion chamber attains a temperature higher than the excess air flowing over its inner vertical walls and the pot outer surface. Therefore, heat is transferred through both convection (Q_{10}) and radiation (Q_{11}) to excess air, whereas pot outer surface receives radiation heat (Q_{12}) from the combustion chamber inner wall as in Eq. 3.4. The excess air flows with velocity V_a and temperature T_{ig} over the combustion chamber inner wall and the related convective heat transfer coefficient could be determined using Eq. 3.28. As the excess air flows through the gap between the flame and the combustion chamber inner wall, the excess air also receives heat from the flame. As flow of both the flame and the excess air depends on the draft created inside the combustion chamber, it is assumed that both the flame and the excess air maintain no relative velocity. Thus, the excess air envelope receives conductive heat (Q_5) from the flame using correlation of Eq. 3.2. The radiation heat (Q_{11}) received by the excess air envelope is a combined effect of both the flame and the combustion chamber inner wall. Both the flame and combustion chamber are considered as diffused and gray surfaces [19] and thus Q_{11} is determined as in Eq. 3.30.

$$Q_{11} = \frac{\sigma A_{CC}(T_f^4 - T_{CC}^4)}{\frac{1}{\varepsilon_f} + \frac{1-\varepsilon_{CC}}{\varepsilon_{CC}}\left(\frac{r_f}{r_{CC}}\right)} \qquad 3.30$$

where,

$$\frac{A_f}{A_{CC}} = \frac{r_f}{r_{CC}} \qquad 3.31$$

where, view factor is considered to be unity, ε_{CC} combustion chamber emissivity and ε_f is the flame emissivity as shown in Eq. 3.29 [13].

The net heat received by the inner wall is therefore conducted through the walls to the combustion chamber outer wall. However the outer wall temperature of the combustion chamber is experimentally determined in order to resemble the original operating condition and determine the skin heat loss. Thus the combustion chamber outer wall losses heat (Q_{13}) through both convection and radiation to the ambient. The convective heat transfer coefficient is obtained from Eq. 3.28.

3.3.5 Modeling output parameters

A comprehensive heat transfer analysis as presented in previous section has been done to model (i) ignition front velocity, (ii) burn rate, (iii) power delivery, (iv) efficiency and (v) time to boil of a biomass cook stove working under steady state of operation. Ignition front velocity (Eq. 3.8), (ii) burn rate (Eq. 3.13) and (iii) power delivery (Eq. 3.14) are presented earlier. The models for efficiency and time to boil are discussed below.

The cooking pot due to its relatively lower temperature receives radiation heat from both flame (Q_8) and fuel bed (Q_9) and is determined using Eq. 3.4. The emissivity of flame near the pot outer surface is determined by Eq. 3.29. On the other hand, as the pot's side surface is exposed to the ambient, heat (Q_{20}) is lost through combined effect of convection and radiation and are determined using Eq. 3.3 and Eq. 3.4. The convective heat transfer coefficient of air over pot's outer surface is determined from Eq. 3.28. Useful heat received by the pot is the sum total of heat from flame (Q_8 and Q_{14}), fuel bed (Q_9), flue gas (Q_{15} and Q_{16}) and combustion chamber (Q_{16}) and losses heat of Q_{20} from its outer surface. Thus, efficiency of the stove is modeled as Eq. 3.32 below.

$$\eta_{stove} = \frac{Q_8+Q_9+Q_{12}+Q_{14}+Q_{15}+Q_{16}-Q_{20}}{\dot{m}\times NCV_f} \quad 3.32$$

Similarly, time to boil is modeled as Eq. 3.33 below

$$Time\ to\ boil = \frac{(m_{w,evap}\times c_{p,w}\times(T_b-T_i))}{Q_8+Q_9+Q_{12}+Q_{14}+Q_{15}+Q_{16}-Q_{20}} \quad 3.33$$

where $\dot{m}$, NCV_f, $m_{w,evap}$, $c_{p,w}$, T_b and T_i are the fuel burn rate, calorific value of fuel, mass of water evaporated, specific heat of water, boiling temperature of water and initial temperature of water.

Heat consumed (Q_{22}) for evaporation is used to estimate mass of water evaporated ($m_{w,evap}$) as provided in Eq. 3.34 and Eq. 3.35 below.

$$Q_{22} = Q_8 + Q_9 + Q_{12} + Q_{14} + Q_{15} + Q_{16} - Q_{20} - Q_{21} \quad 3.34$$

$$m_{w,evap} = Q_{22}/h_{fg} \quad 3.35$$

where Q_{21} is the sensible heat utilized by the water in the pot to reach to the boiling point. The water in the pot, receives heat through a flux of Q_{21}'' from pot bottom at temperature T_{pb} and could be determined using Eq. 3.36 [19].

$$Q_{21}^{"} = \mu_l h_{fg} \left(\frac{g(\rho_l - \rho_v)}{\sigma}\right)^{1/2} \left(\frac{c_{p,l}\Delta T_e}{C_{s,f} h_{fg} Pr_l^n}\right)^3 \quad 3.36$$

$$Q_{21} = Q_{21}^{"} \times A_{p,i} \quad 3.37$$

where, $C_{s,f}$ and n are coefficients depending on combination of water and pot material, and $\Delta T_e = T_{Pb} - T_{sat}$. Thus, heat transferred to the water (Q_{21}) is determined as in Eq. 3.37. The energy balance of the combustion process could be represented as in Eq. 3.38 using which the heat trapped in charcoal (Q_{19}) could be determined.

$$Q_{com} = Q_1 + Q_2 + Q_3 + Q_4 + Q_5 + Q_6 + Q_7 + Q_8 + Q_9 + Q_{14} + Q_{15} + Q_{16} + Q_{17} + Q_{18} + Q_{19} \quad 3.38$$

3.3.6 Model implementation and validation

A commercially available stove (*Harsha* stove) is considered for implementation of the models described above. Implementation of the models to estimate five specific outputs concerning performance of biomass cook stove requires data [1-2] concerning seven sub-systems related to its operation as listed in Table 3.3.

Table 3.3**:** Steady state input values to the model

Sl. No	Sub-system	Parameters	Unit	Value	Ref.
1	Ambient conditions	Temperature	K	300	[1]
		Air velocity [a]	m/s	0.5	
2	Pot	Diameter	m	0.26	[20]
		Height	m	0.1	
		Thickness	m	0.0015	
		Material		Aluminum	
		Emissivity		ε = 0.07	
3	Stove	Stove		Harsha Stove	
		Combustion chamber dimensions	m	0.2×0.2× 0.105	[1]
		Stove inclination	°	90	[1]
		Combustion chamber material		Mild steel	
		Combustion chamber material emissivity		ε = 0.2	
		Mode of primary air supply		Natural draft	
		Pot bottom and stove top area	m^2	3.51×10^{-2}	

Sl. No	Sub-system	Parameters	Unit	Value	Ref.
		Fuel Type		Solid biomass	
		Applications		Cooking, heating	
		Number of pots		1	
		Portability		Portable	
		Combustion mode		Top ignition	
		Outer body temperature	K	673.15	Experimental
4	Fuel bed	Dimensions	m	0.2×0.2×0.005[b]	
		Bed emissivity		0.82	[1]
		Bulk density	kg/m^3	250	[1]
		Bed height	m	1.5×10^{-2}	
		Particle density	kg/m^3	1020	[1]
		Specific heat of particle	J/kg K	4187	
		Vapour temperature	K	373	
		Latent heat of vapourization	J/kg	2441000	
		Air density	kg/m^3	1.16	
5	Flame	Thickness	m	0.19	
		Height	m	0.1	
		Cross-sectional area	m^2	3.94×10^{-2}	
		Side surface area	m^2	5.27×10^{-2}	
		Decay coefficient	m^{-1}	7.32×10^{-1}	[13]
		Natural draft convective heat transfer coefficient	W/m^2K	28.39	[13]
6	Fuel properties	Proximate analysis	%	Volatiles=74% Moisture=10% Fixed carbon=15% Ash =1%	[1]
		Ultimate analysis	%	C=52.9%, H_2=6.3C%, N_2=0.1%, O_2=39.7%, Ash=1%	
		Calorific value	J/kg	17425950	
		Particle dimensions	m	0.015×0.015×0.015	[1]
		Thermal conductivity	W/mK	0.17	
		Ignition temperature	K	650	[1]
7	Saturated water properties at 373.15 K	Boiling temperature	K	373.15	[19]
		Density	kg/m^3	957.9	
		Specific heat	J/kg K	4217	
		Viscosity	Ns/m^2	2.79×10^{-4}	
		Prandtl number		1.76	
		Latent heat of vaporization	J/kg	2257000	
		Surface tension	N/m	5.89×10^{-2}	
	Saturated water vapor properties at 373.15 K	Density	kg/m^3	5.95×10^{-1}	
		Acceleration due to gravity	m/s^2	9.8	

[a] Assumed wind velocity.

[b] Steady state is obtained at assumed bed height.

The input values pertaining to ambient, pot, stove physical properties, fuel bed and fuel properties are obtained from literature [1] corresponding to test condition under similar

operating conditions as mentioned in literature for evaluation of the stove's performance. Input parameters of flame and water are considered according to the standard literatures [13, 19].

Further, heat transfer model uses the design features of Harsha stove to deliver ignition front velocity, burn rate and power delivery as per the test conditions [1]. The performance parameters i.e. efficiency and time to boil from the simulated model are further compared with the experimentally obtained results [21-25]. The heat transfer model uses the Water Boiling Test conditions for simulation [26].

3.4 Results and discussions

3.4.1 Flame temperature and power delivery of stove

The combustion chamber of the stove accommodates a fuel bed of 4×10^{-2} m^2 cross-sectional area and has 196 ducts of 2.01×10^{-6} m^2 cross-sectional area. The *Harsha* stove operates at an ignition front velocity of 3.8×10^{-5} m/s and creates a flame of temperature 1003.75 K. The air is sucked with a flow rate of 1.2×10^{-3} m^3/s through the gaps with fuels burning at the rate of 3.77×10^{-4} kg/s and power output of 6.58 kW. The operating parameters considered for SHTM are listed in Table 3.4.

Table 3.4**:** Steady state fuel bed and flame conditions for steady state heat transfer modeling

	Ignition front velocity	**Air flow rate at gaps**	**Flame temperature**	**Burn rate**	**Average power delivery**	**Ref.**
	mm/s	**m^3/s**	**K**	**kg/s**	**kW**	
Model value	0.038	0.0012	1003.75	3.77×10^{-4}	6.58	
Reported value	0.038	0.0014	1133.15[a]	3.8×10^{-4}	5.6, Maximum instantaneous = 14.1	[1]

3.4.2 Heat transfer analysis of fuel bed

The fuel bed of the stove for the present study is divided into two parts i.e. top igniting layer of thickness equal to the height of a single particle i.e. 1.5×10^{-2} m and rest of fuel bed height as bottom fuel bed. During steady state the top fuel bed maintains a temperature of 826.87 K which is the average of flame temperature (1003.75 K) and

ignition temperature (650 K). The bottom fuel bed whereas maintains a temperature of 563.43 K which is the average of ambient and top bed temperature.

The combustion air passes through bottom fuel bed gaps at 1.6×10^{-2} m/s and receives 2.28 W (Q_{4a}) heat to raise its temperature to 650 K. The values for n_{N_2} and n_{O_2} is obtained as 0.45 and 6.7×10^{-2} respectively. The air then passes through the top igniting layer with Nusselt number of 6 [12] which in turn results in heat transfer coefficient of 203.96 W/m^{2}K. As a result the combustion air receives a total of 606 W (Q_1) from the top igniting fuel bed.

The combustion air after passing through the gaps gets divided into two parts i.e. air used in combustion and excess air. From the supplied air, about 3.25×10^{-8} m^3/s of air is used for combustion whereas remaining 4.70×10^{-10} m^3/s is excess air. During steady state as the flow is continuous, the air for combustion continuously forms a layer over the fuel bed whereas the excess air forms an air envelope around the flame. The air used in combustion forms a thin layer of 8.25×10^{-7} m thickness above the cross-sectional area of the fuel bed and below the flame formation zone before mixing with the volatiles. In this region the combustion air again receives heat of 529.77 W (Q_2) from the fuel bed. Thus, a total of 1135.87 W (Q_1+Q_2) is received by the combustion air before taking part in combustion.

Subsequently, an amount of 118 W (Q_4) heat is transferred by the top fuel bed igniting layer to the bottom fuel bed of the fuel bed. However during steady state the bottom fuel bed maintains a relatively higher temperature than the surrounding ambient, which results in heat loss of 169.91 W (Q_{4b}) through the grate. In a subsequent process, the bottom fuel bed also losses heat to evaporate the moisture in the fuel. Thus an amount of 92.20 W (Q_{4c}) is utilized to remove moisture of 3.77×10^{-5} kg/s from the fuel bed during steady state.

Similarly, the fuel bed transfers 327.56 W (Q_7) and 415 W (Q_9) to the combustion chamber (738.43 K) and pot (cross-sectional area of 5.3×10^{-2} m^2 and at 378.15 K) respectively through radiation mode with view factors of 0.49 and 0.50 respectively. The remaining 1611 W (Q_{19}) heat is trapped as unburned charcoal i.e. formation of 5.39×10^{-5} kg/s charcoal having calorific value of 30×10^6 J/kg.

3.4.3 Heat transfer analysis of flame

As the ignition propagates the fuel bed starts releasing volatiles which forms a volatiles rich region at the top of the fuel bed and combustion air layer. In the present study the volatiles forms a layer of thickness 1.42×10^{-3} m which on mixture with the high temperature air forms the flame. Thus the flame transfers heat of 554 W and 140 W through both conduction and radiation respectively to the top surface of fuel bed and sums to an amount of 694 W (Q_3). The flame maintains a view factor of 0.98 and has an emissivity of 0.46, decay coefficient as 0.7322 m^{-1} and flame thickness equal to fuel bed diameter of 0.19 m.

The excess air which doesn't take part in combustion thus forms a 1.4×10^{-3} m thick envelope around the flame. As flow of excess air and flame are both dependent on the pressure drop inside the combustion chamber therefore the relative velocity between them is considered negligible. Thus the excess air receives heat of 649 W (Q_5) through conduction mode from the flame. Moreover as the combustion chamber and the pot bottom both surround the flame therefore they receive heat of 77 W (Q_6) and 50 W (Q_8) through radiation from the flame. However as the excess air is enclosed within both the combustion chamber at 738.43 K and flame therefore it also receives heat through radiation. For determination of the amount of heat radiated both the flame and combustion chamber inner surfaces are considered to be diffused and gray radiators with emissivity of 0.2 and 0.35 respectively. Therefore the excess air envelope receives radiation heat of 336 W (Q_{11}) due to combined effect of flame and combustion chamber.

The flame after passing through the combustion chamber comes in contact with the pot bottom surface of 5.30×10^{2} m^2 and therefore transfers convective heat of 1061 W (Q_{14}). However as the flame comes in contact with the cold surface of the pot the flame temperature drops and results in formation of unburned particles. The rest of the flame which burns completely, along with the excess air and unburned particles forms the flue gas at 690.95 K. The flue gas thus formed makes contact with the pot's outer surface with a velocity of 1.6×10^{-4} m/s. The resulting flue gas Reynold's Number, Prandtl Number and Nusselt Number are 0.33, 0.73 and 0.37 respectively which results in convective heat transfer coefficient of 0.14 W/m^2K over the pot's side surface. Thus

convective heat of 2.35 W (Q_{15}) and 3.94 W (Q_{16}) is received by the pot bottom and pot side surface respectively from the flue gas.

The flame while transferring heat to the pot's outer surface gets exposed to the ambient and therefore losses 98.39 W (Q_{17}) heat. Simultaneously, the flue gas after transferring heat to the pot carries heat of 3 W (Q_{18}) along with it to the ambient.

3.4.4 Heat transfer analysis of combustion chamber

The combustion chamber inner surface as it surrounds the flame and fuel bed maintains a relatively higher temperature of 738.43 K as compared to the excess air at 650 K and pot bottom at 378.15 K. The excess air envelope, as discussed already, flows in a laminar profile over the inner surface of the combustion chamber with a velocity of 1.6×10^{-4} m/s. During its flow over the combustion chamber inner surface, the air receives convective heat of 1.21 W (Q_{10}) in addition to radiation heat as discussed already as Q_{11}.

Also the combustion chamber transfers heat of 82.07 W (Q_{12}) through radiation to the pot bottom with view factor of 0.31. Although the rest of heat transferred to the combustion chamber outer wall could be determined through heat balance, however the outer surface temperature could not be determined as the duration of operation is not considered. In order to determine the heat loss from the combustion chamber outer wall experimentally obtained temperature of stove's outer wall i.e. 673.15 K is considered. Thus about 261.97 W and 187.87 W of convective and radiation heat respectively is lost from the outer surface, accounting to a total of 449.84 W (Q_{13}).

3.4.5 Heat transfer analysis of pot

The pot as discussed, during consideration of steady state receives a total of 1532 W from flame (Q_8 and Q_{14}), fuel bed (Q_9) and flue gas (Q_{15} and Q_{16}). However as the pot's outer surface maintains a relatively higher temperature of 378.15 K as compared to ambient temperature of 300 K, heat of 58.67 W (Q_{20}) (convection loss: 54.67 W and radiation loss: 4.00 W) is lost to the ambient. Thus the water receives a net heat of 1555.40 W considering energy balance between heat received and lost.

The pot inner surface in turn transfers an amount of 227.10 W (Q_{21}) to boil the water at a net heat flux of 4277.55 W/m^2, whereas the rest of the heat i.e. 1328.29 W (Q_{22})

obtained through energy balance is lost in evaporation. The heat utilized in evaporation thus results in evaporation of water at the rate of 5.88×10^{-4} kg/s.

3.4.6 Distribution of thermal energy components within biomass cook stove

Eighteen components out of the total 22 components as discussed above are directly related with the design and operation of the cooking stove. Distribution of these estimated components are presented in Fig. 3.2 and Fig. 3.3 which are discussed below.

The rate of heat released during the operation of the stove is estimated at about 6583 W out of which about 55% is contributed by fuel bed (3611 W) and 45% by flame (2972 W). Heat from the fuel bed is subsequently transferred to air passing through it (1136 W, 17.25%) and heat radiated to pot (416 W, 6.31%) combustion chamber (328 W, 4.98 %) and bottom fuel bed (118 W, 1.79%).

Similarly, the rates of thermal energy transfer from flame to the pot (1110 W, 16.86%), excess air (985 W, 14.96%), fuel bed (693 W, 10.53%), surrounding (98 W, 1.49%) and combustion chamber (77 W, 1.16%) have a variation due to the variability of the system parameters.

Total amount of heat transferred to air from fuel bed and flame accounts for about 2121 W. Reduction of this component of heat through arrangement of air pre-heating would enhance the efficiency. Further, about 1613 W heat is trapped in charcoal and may be lost as unutilized. The unburned fuel is a characteristic of natural draft stove due to inadequate air supply.

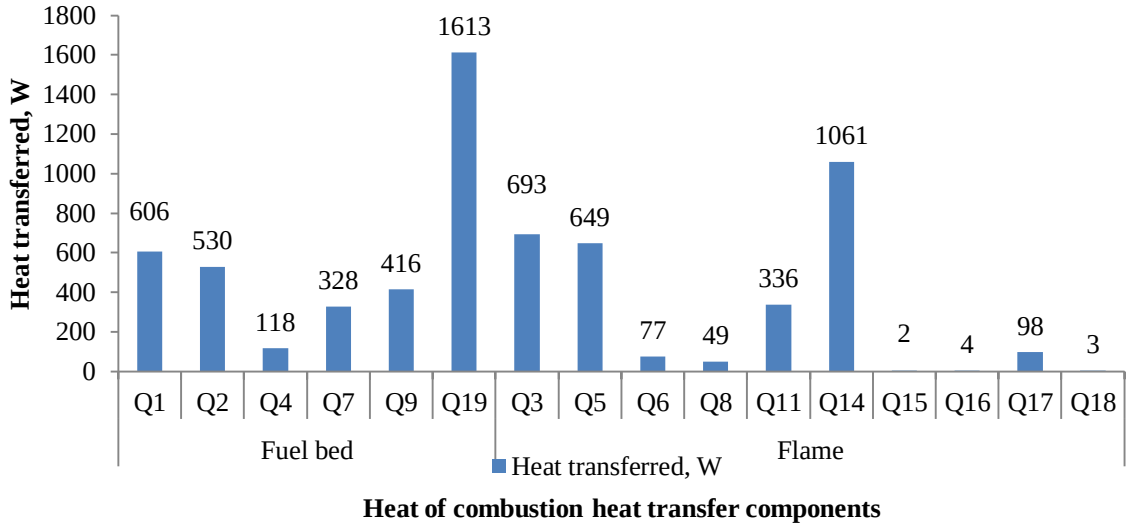

Fig.3.2. Heat transfer analysis of heat of combustion

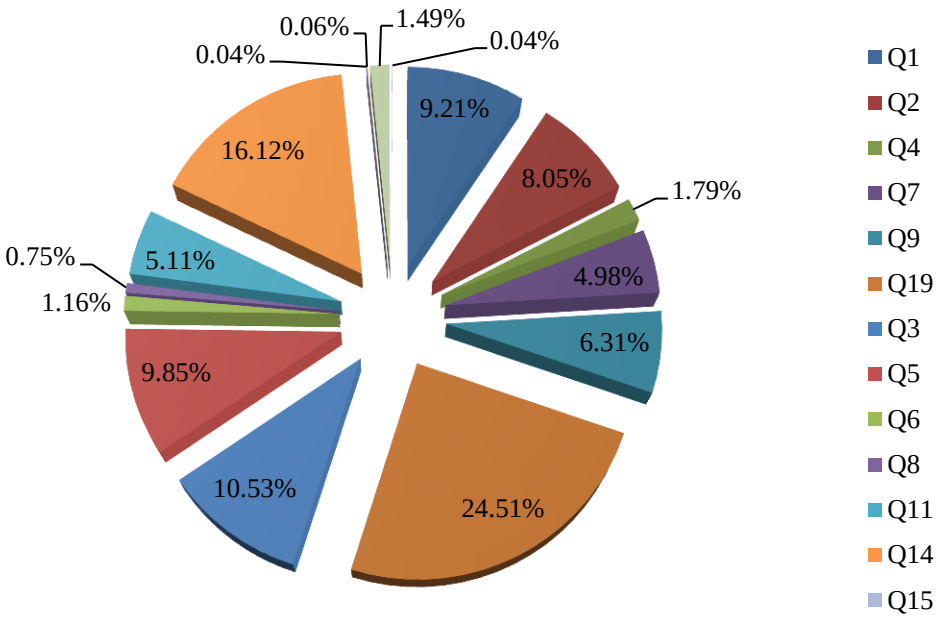

Fig. 3.3 Share of each component on heat of combustion

3.4.7 Performance analysis and validation

As mentioned in the previous section, *Harsha* stove is modeled for assessment of its performance through standard performance parameters of (i) ignition front velocity, (ii) burn rate, (iii) power delivery, (iv) efficiency and (v) time to boil. Maximum instantaneous power delivery of the stove has been estimated as 6.58 kW with 1003.75 K flame temperature at ignition front velocity of 3.8×10^{-5} m/s.

Table 3.5: Steady state heat transfer model validation

	Efficiency	**Time to boil**	**Ref.**
	%	**Min**	
Reported values	26.10-26.80	15.5	[21]
	24.80		[22]
	28.60		[23]
	24.80		[24]
	28.60		[25]
SHTM value	23.63	16.94	

The stove operates with estimated 23.63% efficiency and requires about 17 minutes to boil 5 litres of water. As could be observed from Table 3.5 the experimental values of *Harsha* stove has been reported with variations in burn rate, overall power delivery

and efficiency [21-22, 24-26]. The values predicted for *Harsha* stove are found comparable with the experimental values and thus validates the SHTM.

3.5 Summary

In the present chapter a biomass fuelled cook stove i.e. *Harsha* stove is modeled through a steady state heat transfer model. A delineated heat transfer model comprising key parameters (designing, operating and performance parameters) of stove is developed through application of fundamental heat transfer relationships. A total of 22 different and distinct heat transfer components could be modeled in terms of above parameters. Such delineated knowledge was not available earlier. The developed heat transfer model has enhanced the understanding of stove's working and dependence of performance on operating and designing parameters. Identification of the status (useful or loss) of each heat transfer component has helped the designers in optimally designing a stove and incorporate modifications to minimize losses. Incorporating air preheating, forced draft, flue gas waste heat recovery and minimize charcoal formation could improve the performance of biomass stove. Absence of these parameters could be quantified.

REFERENCES

[1] Kausley, S. B., and Pandit, A. B. Modelling of solid fuel stoves. *Fuel*, 89(3): 782-791, 2010.

[2] Saastamoinen, J. J., Taipale, R., Horttanainen, M., and Sarkomaa, P. Propagation of the ignition front in beds of wood particles. *Combustion and flame*, 123(1-2): 214-226, 2000.

[3] Raman, P., Ram, N. K., and Murali, J. Improved test method for evaluation of biomass cook-stoves. *Energy*, 71: 479-495, 2014.

[4] Guo, B., Li, D., Cheng, C., Lü, Z.A. and Shen, Y. Simulation of biomass gasification with a hybrid neural network model. *Bioresource Technology*, 76(2): 77–83, 2001.

[5] Brown, D., Fuchino, T., Maréchal, F. Solid fuel decomposition modelling for the design of biomass gasification systems. Computer Aided Chemical Engineering, 21:1661–66. 2006

[6] Sedighi, M., and Salarian, H. A comprehensive review of technical aspects of biomass cookstoves. *Renewable and Sustainable Energy Reviews*, 70: 656-665, 2017.

[7] Xue, Q., Heindel, T. J., and Fox, R. O. A CFD model for biomass fast pyrolysis in fluidized-bed reactors. *Chemical Engineering Science*, 66(11): 2440-2452, 2011.

[8] Fernando, N., Amin, M., Narayana, M., Jayawickrama, T., and Jayasena, S. A. A mathematical model for Pyrolysis of biomass. In *Moratuwa Engineering Research Conference* (MERCon-2015), pages 6-11, Moratuwa, Sri Lanka, April 7-8, 2015. IEEE.

[9] Sutar, K.B., Kohli, S., Ravi, M.R., and Ray, A. Biomass cookstoves: A review of technical aspects. *Renewable and Sustainable Energy Reviews*, 41: 1128-1166, 2015.

[10] Urmee, T., and Gyamfi, S. A review of improved Cookstove technologies and programs. *Renewable and Sustainable Energy Reviews*, 33: 625-635, 2014.

[11] Wijeysundera, N. E. *Engineering Thermodynamics with Worked Examples*. World Scientific, Singapore, 2nd edition, 2017.

[12] Morini, G.L. Thermal characteristics of slug flow in rectangular ducts. *International journal of thermal sciences*, 38(2): 148-159, 1999.

[13] Welker, J. R., and Sliepcevich, C. M. Heat Transfer by Direct Flame Contact Fire Tests. Phase I. *National Academy of Sciences Washington DC Committee on Hazardous Materials*, 1971.

[14] Leuenberger, H. and Person, R.A. Compilation of radiation shape factors for cylindrical assemblies. *The American Society of Mechanical Engineers*. 1960.

[15] Pastor Ferrer, E., Rigueiro, A., Zárate López, L., Gimenez, A., Arnaldos Viger, J., and Planas Cuchi, E. Experimental methodology for characterizing flame emissivity of small scale forest fires using infrared thermography techniques. In *IV International Conference on Forest Fire Research 2002 Wildland Fire Safety Summit*, 1-11, 2002.

[16] Culham, J. R., Yovanovich, M. M., Teertstra, P., Wang, C.S., Refai-Ahmed, G., and Tain, R.M. Simplified analytical models for forced convection heat transfer from cuboids of arbitrary shape. *Journal of Electronic Packaging*, 123(3): 182-188, 2001.

[17] *Flue gas properties table.* Retrieved on 12 Apr, 2017 from https://www.pipeflowcalculations.com/tables/flue-gas.xhtml, 2017.

[18] Sartori, E. Convection coefficient equations for forced air flow over flat surfaces. *Solar Energy*, 80(9): 1063-1071, 2006.

[19] Incropera, F. P., and Dewitt, D. P. *Fundamentals of heat and mass transfer*, Wiley-India Edition, 5th edition, 2009.

[20] Indian standard, Portable Solid Bio-mass Cookstove (chulha) (First revision) IS 13152 (Part 1): 2013, Bureau of Indian Standards, Aug. 2013. Retrieved on 23 Apr. 2016 from http://www.newdawnengineering.com/website/library/Stoves/Stove%20Testing/Testing%20Protocols/India/BIS%20stove%20test%20Feb%202014.pdf, February 2014.

[21] Bhattacharya, S. C., Albina, D. O., and Khaing, A. M. Effects of selected parameters on performance and emission of biomass-fired cookstoves. *Biomass and Bioenergy*, 23(5): 387-395, 2002.

[22] Bansal, M., Saini R. P., and Khatod, D. K. Development of cooking sector in rural areas in India-A review. *Renewable and Sustainable Energy Reviews***,** 17: 44-53, 2013.

[23] Mehetre, S.A., Panwar, N.L., Sharma, D., and Kumar, H. Improved biomass cookstoves for sustainable development: A review. *Renewable and Sustainable Energy Reviews*, 73: 672-687, 2017.

[24] Indian improved cookstoves: A compendium, Food and Agriculture Organization of the United Nations, Bangkok, July, 1993. Retrieved on 10 Apr. 2019 from http://www.fao.org/3/AD585E/ad585e00.pdf, 1993.

[25] Approved models of portable improved biomass cookstoves. Retrieved on 10 Apr. 2019 from https://mnre.gov.in/file-manager/UserFiles/approved-models-of-portable-improved-biomass-cookstove-manufactures.pdf, 2013.

[26] The Water Boiling Test, Version 4.2.3, Cookstove Emissions and Efficiency in a controlled Laboratory Setting, March, 2014. Retrieved on 15 Mar. 2017 from https://www.cleancookingalliance.org/binary-data/DOCUMENT/file/000/000/399-1.pdf, 2014.